EPJ Web of Conferences **119**, 26002 (2016) DOI: 10.1051/epjconf/201611926002
ILRC 27

INTEGRATED PATH DETECTION OF CO_2 AND CH_4 USING A WAVEFORM DRIVEN ELECTRO-OPTIC SINGLE SIDEBAND LASER SOURCE

Gerd Wagner[1], Stephen Maxwell[2], David Plusquellic[1*]

*[1]Quantum Electronics and Photonics Division, Physical Measurement Laboratory, National Institute of Standards and Technology, Boulder, CO 80305, USA, *Email: david.plusquellic@nist.gov*
[2]Sensor Science Division, Physical Measurement Laboratory, National Institute of Standards and Technology, Gaithersburg, MD 20899, USA

ABSTRACT

Integrated path concentrations of ambient levels of carbon dioxide and methane have been measured during nighttime periods at NIST, Boulder (CO, USA), using a ground-based, eye-safe laser system. In this contribution, we describe the transmitter and receiver system, demonstrate measurements of CO_2 and CH_4 in comparison with an *in situ* point sensor measurement using a commercial cavity ring-down instrument, and demonstrate a speckle noise reduction method.

1. INTRODUCTION

Differential absorption lidar (DIAL) is an active remote sensing technique for measuring range-resolved concentrations of trace gases, e.g., CO_2, CH_4, and H_2O in the atmosphere. The integrated path differential absorption (IPDA) method is similar to DIAL except that it uses natural or mirror surface reflections from hard targets to determine the column concentrations of trace gases in the atmosphere. IPDA can achieve much higher signal-to-noise (SNR) ratio compared to DIAL due to the 100% duty cycle and large return signals from surface reflection. DIAL and IPDA are advantageous compared to passive remote sensing instruments using Fourier-transform infrared (FTIR) and microwave (MW) methods. First, active remote sensing achieves a higher SNR compared to passive remote sensing methods. Second, aspects of DIAL and IPDA instruments are self-calibrating due to their measurement principle. Third, given sufficient power, active remote sensing measurements can be performed during night and day times.

The paper is structured as follows. Section 2 introduces the experimental setup of the NIST IPDA system and its specifications. Section 3 describes the theoretical modeling of the absorption line and the nonlinear fitting routine of the experimental data. IPDA measurements of CO_2 + H_2O and CH_4 + H_2O in comparison with an *in situ* point sensor are presented in Section 4. A speckle noise reduction method is introduced in section 5. A summary with an outlook is given in section 6.

2. NIST IPDA SYSTEM SETUP [1]

The experimental setup of the IPDA system is depicted in Fig. 1 and is based on [2]. A single mode external cavity diode laser (ECDL) tunable from 1585 nm to 1646 nm is launched into a polarization maintaining (PM) single mode fiber, coupled through two isolators to minimize optical feedback and split into two paths using a fiber splitter with a 90% : 10% ratio to provide signals for the scan leg and lock leg, respectively.

The lock leg is coupled to an electro-optic phase modulator (EOM) and then to an acousto-optic modulator (AOM). The EOM is driven at 15 MHz to provide sidebands for stabilization of the ECDL to the filter cavity. The AOM is driven at 251.73 MHz (250 MHz center frequency) with a Rubidium (Rb) referenced radio frequency (RF) source to provide a frequency offset for sideband selection of the scan leg. The output is coupled through a circulator and free space launched through a polarizing beam splitter (PBS) and mode matched to the filter cavity. The signal from a 150 MHz bandwidth photodiode that monitors the reflected beam from the circulator (CIR) is mixed with the 15 MHz reference and demodulated for stabilization (Pound-Drever-Hall (PDH) stabilization technique) [3].

The scan leg is amplified to 20 mW using a semiconductor optical amplifier, and coupled to a broadband EOM (EOM2) to provide sidebands for frequency tuning. EOM2 is driven by an arbitrary

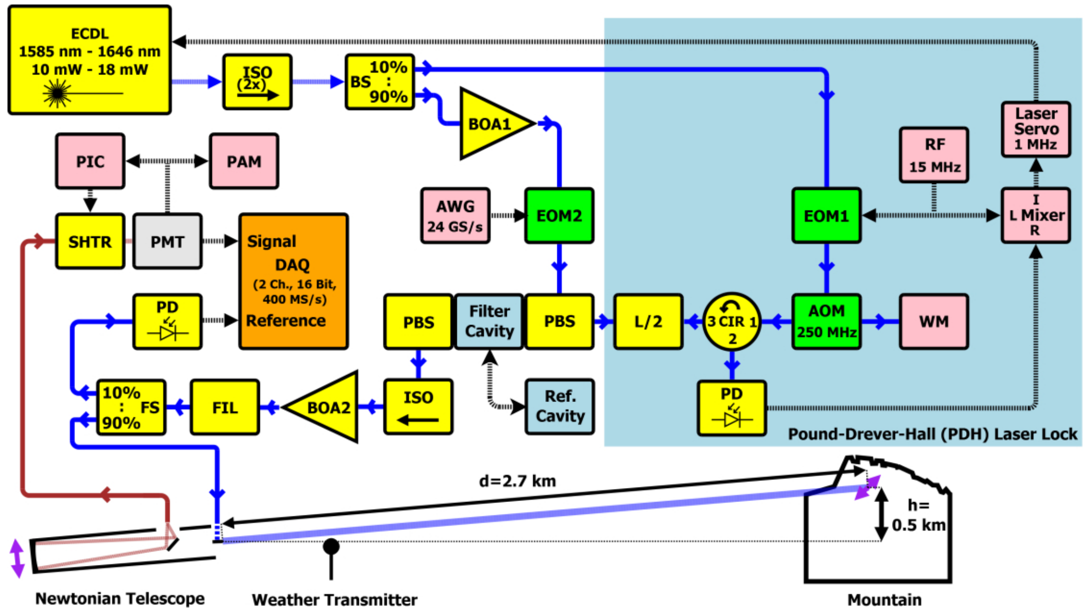

Figure 1. NIST IPDA system setup (PAM, picoammeter; PIC, PMT protection circuit; WM, HeNe reference).

waveform generator (AWG) having 10 GHz of bandwidth (interleaved clock rate of 24 GigaSamples/s (GS/s)). The PDH error signal is conditioned in a 10 MHz band-pass proportional-integral-differential (PID) gain controller and the PID output is limited to < 1 MHz bandwidth to drive the diode laser current for stabilization to the filter cavity. The lock stability of the laser relative to the filter cavity is estimated at < 200 kHz from the noise content of the error signal.

The filter cavity is a linear confocal resonator with a transverse mode spacing of 150 MHz (cavity length is 0.5 m) and a cavity finesse of 43 (mirror reflectivity R=93%). For the transmission and rapid tuning of the 2nd order EOM sideband, the AOM frequency determines the MW tuning frequencies and filter properties of the cavity. An AOM frequency near 250 MHz is used to give sideband and carrier rejection of the scan leg through 3rd order. After mode matching, the resonant contribution of the 4th order sideband is typically less than 0.5% of the 2nd order power.

An absolute frequency reference for the diode laser was achieved by locking the zero-order beam from the AOM (with 15 MHz sidebands) to an optical reference (transfer) cavity. The reference cavity is actively locked to a polarization-stabilized HeNe laser using a piezo-electric transducer (PZT) and heater with a long term absolute frequency stability of better than ± 0.5 MHz. Since the laser is frequency locked to the filter cavity, slow feedback corrections (with a 0.1 s time constant) to the laser frequency are indirectly enforced by controlling the filter cavity length using the PZT driven cavity mirror.

The free space output of the filter cavity is coupled back into a PM fiber, fed through an optical isolator and amplified using a booster amplifier (BOA2). BOA2 is driven near saturation with up to 27.5 mW of continuous wave output power. Due to amplified spontaneous emission (ASE), the output of BOA2 is filtered with an optical bandpass (FIL, 12 nm FWHM, 70% transmission) and split using a 90% : 10% fiber splitter. The 10% leg is used for the initial power leveling at each of the 123 step frequencies, and for the long-term power normalization of the remote sensing signals. The power of the 90% leg is < 9.5 mW (an eye-safe level) and is coupled to the transmitter mounted on the telescope receiver.

The transmitter unit consists of a fiber collimator and a (1:5) beam expander resulting in an output beam diameter of 1.9 cm (1/e^2 beam diameter).

A 25 cm Newtonian–type telescope (currently being updated to a 28 cm Schmidt-Cassegrain-type telescope) is used as a receiver. The IPDA return signal is collected at the telescope focus using a multimode fiber with diameter, d = 550 μm or 910 μm, numerical aperture, NA = 0.22, and coupled to a photomultiplier tube (PMT) with a quantum efficiency of 3% at 1600 nm, and 0.3% at 1645 nm.

For photon counting, a preamplifier-amplifier-discriminator setup is used to generate a 5.0 ns output pulse for each electron pulse from the PMT above a discriminator threshold. A 16-bit analog-to-digital converter (ADC) is used to digitize two channels at a combined rate and throughput of 400 MegaSamples/sec (MS/s). Channel 1 is used to monitor the discriminator output and to count photons (signal channel), and channel 2 is used to digitize a 100 MHz InGaAs photodiode used to monitor the reference power.

Figure 2 shows the signal and reference channel with the 123 frequencies (pulse width is 600 ns at each frequency). Each scan consists of 123 frequencies and takes 0.1 ms to acquire (scan repetition rate is 10 kHz).

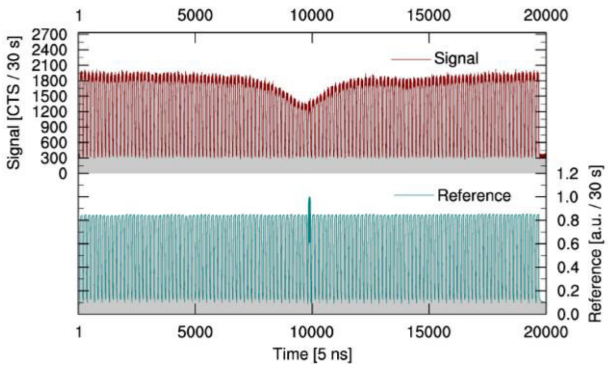

Figure 2. Signal and reference channels. The central dip in signal channel is due to ambient CO_2 and the dip on the right shoulder is water vapor.

3. ABSORPTION LINE MODELING

The atmospheric transmission model to retrieve the column-integrated trace gas concentrations is based on the sum of Voigt line shapes generated from the information contained in the HITRAN 2008 [4] for CH_4 and HITRAN 2012 [5] database for CO_2 and H_2O. A weather transmitter located near the start of the optical path provides initial environmental conditions for the model. Since the optical path is extended over an elevation of 500 m (see Section 4), the line shape model that is fit to the data is first integrated over a set of temperature and pressure range bins. The experimental absorption data is fit to the model line using the Levenberg–Marquardt algorithm [6].

4. IPDA MEASUREMENTS OF CO_2 AND CH_4

IPDA nighttime measurements of CO_2 and CH_4 have been performed from January to March 2015 at NIST, Boulder (CO, USA). The IPDA system was located inside a NIST lab and was pointing towards a rock formation (a Flatiron mountain face) at a distance of 2.7 km and over a difference in altitude of 500 m. Figures 3, 4 show NIST IPDA measurements of CO_2 and CH_4, respectively, in comparison with the *in situ* cavity-ring down measurements (Picarro G2301). For most of these nighttime runs, water vapor was also fit as a shoulder feature but not shown here. Corrections for dry air concentrations are underway.

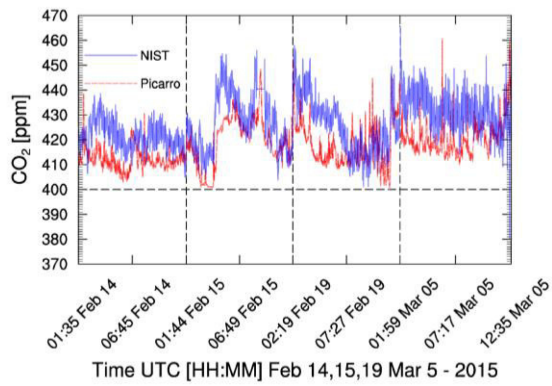

Figure 3. IPDA nighttime data of CO_2 at 1602 nm.

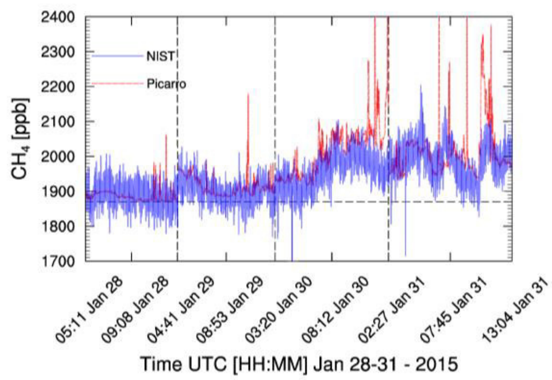

Figure 4. IPDA nighttime data of CH_4 at 1645 nm.

5. SPECKLE NOISE REDUCTION

Speckle is the main source of noise in the IPDA measurement signals [7]. A method of reducing speckle noise is achieved by spatial averaging to remove the temporal coherence over a large number of speckle cells (currently > 30,000). During IPDA signal acquisition, we rapidly modify the pointing position of the telescope. The telescope is slewed repeatedly by ± 1 deg. over a 40 m x 0.4 m area of the target every 4 sec. A galvanometer scanner also moves the transmitted beam within the field of view of the telescope perpendicular to the slewing direction of the telescope at a repetition rate of 50 Hz.

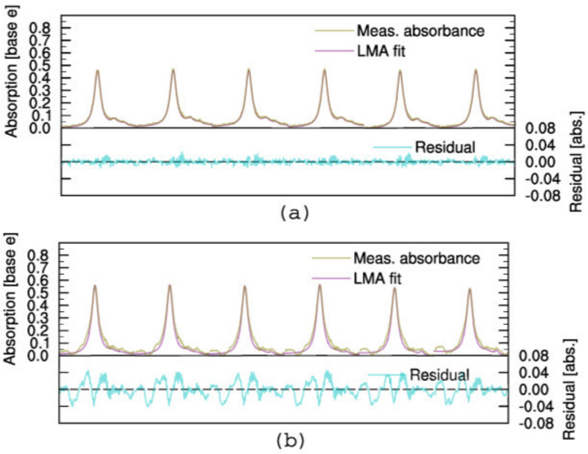

Figure 5. (a) Speckle reduction by moving telescope, (b) speckle with stationary telescope.

Figure 5 shows a comparison of an IPDA absorption measurement of CO_2 at 1602 nm with (a) and without (b) speckle noise reduction, respectively. The signals are shown for 6 consecutive absorption intervals, each averaged for a 30 s period (300,000 scans). As evident in the residuals, this method removes a significant fraction of the systematic error associated with the baseline features. For CO_2 data in Figure 5a, the statistical uncertainty in fitted concentration per interval is near 0.5 %, which is still more than a factor of 5 larger than the quantum (Poisson) noise floor.

6. SUMMARY AND OUTLOOK

In this contribution, we have presented the setup of the NIST IPDA system and showed IPDA measurements of CO_2 and CH_4 in comparison with *in situ* results from a commercial cavity-ring down instrument. We demonstrated a significantly reduce systematic error associated with speckle. For CO_2 retrievals, the addition of a fiber amplifier is planned to permit day time data acquisition. The IPDA system will be used for comparison of CO_2 and CH_4 retrievals obtained using range-resolved DIAL that is under development.

ACKNOWLEDGEMENT

The NIST Greenhouse Gas Measurement Initiative provided financial support. The Picarro G2301 analyzer was kindly loaned by Colm Sweeney and Anna Karion (NOAA Earth System Research Laboratory, Global Monitoring Division, Boulder CO). We also wish to thank Alan Brewer (NOAA Chemical Sciences Division, Boulder CO) for assistance with the transmitter alignment.

REFERENCES

[1] Certain equipment, instruments or materials are identified in this paper in order to adequately specify the experimental details. Such identification does not imply recommendation by the National Institute of Standards and Technology nor does it imply the materials are necessarily the best available for the purpose.

[2] Douglass, K. O., S. E. Maxwell, G.-W. Truong, R. D. van Zee, J. R. Whetstone, J. T. Hodges, D. A. Long, D. F. Plusquellic, 2013: Rapid scan absorption spectroscopy using a waveform-driven electro-optic phase modulator in the 1.6-1.65 µm region, JOSA B, **30**, 2696-2703.

[3] Drever, R. W. P., J. L. Hall, F. V. Kowalski, J. Hough, G. M. Ford, A. J. Munley, H. Ward, 1983: Laser phase and frequency stabilization using an optical resonator, Appl. Phys. B, **31**, 97-105.

[4] Rothman, L. S., and 41 co-authors, 2009: The HITRAN 2008 molecular spectroscopic database, J. Quant. Spectrosc. Ra., **110**, 533-572.

[5] Rothman, L. S., and 48 co-authors, 2013: The HITRAN 2012 molecular spectroscopic database, J. Quant. Spectrosc. Ra., **130**, 4-50.

[6] Moré, J. J., 1978: The Levenberg-Marquardt algorithm: implementation and theory, Numerical Analysis, Lecture Notes in Math., **630**, 105-116.

[7] Ehret, G., C. Kiemle, M. Wirth, A. Amediek, A. Fix, S. Houweling, 2008: Space-borne remote sensing of CO_2, CH_4, and N_2O by integrated path differential absorption lidar: a sensitivity analysis, Appl. Phys. B, **90**, 593-608.